# Explainable Artificial Intelligence for Antenna Sensor Modeling

### Wenkai Tan

Department of Information System University of Maryland, Baltimore County Maryland, USA wtan1@umbc.edu

# Jayaprakash B. Shivakumar

Department of Electrical Engineering&Computer Science Embry-Riddle Aeronautical University Florida, USA shivakuj@my.erau.edu

# Rishikesh Srinivasaraghavan Govindarajan

Department of Aerospace Engineering Embry-Riddle Aeronautical University Florida, USA srinivr1@my.erau.edu

## Nicholas Reed

Department of Aerospace Engineering Embry-Riddle Aeronautical University Florida, USA reedn4@my.erau.edu

#### Daewon Kim

Department of Aerospace Engineering Embry-Riddle Aeronautical University Florida, USA kimd3c@erau.edu

# Eduardo Rojas

Department of Electrical Engineering&Computer Science Embry-Riddle Aeronautical University Florida, USA rojase1@erau.edu

# Yongxin Liu

Department of Mathematics Florida, USA liuy11@erau.edu

# **Houbing Song**

Department of Information System Embry-Riddle Aeronautical University University of Maryland, Baltimore County Maryland, USA songh@umbc.edu

Abstract—The extensive application of Artificial Intelligence and Machine Learning is notable in additive manufacturing realms such as manufacturing supervision and error identification. Nonetheless, the escalating employment of AI in vital processes during production necessitates its decision-making and prediction abilities to display interpretability. Consequently, the need for explainable Artificial Intelligence (xAI) in such manufacturing procedures becomes paramount.

In this paper, we develop an explainable AI framework for antenna sensor modeling during additive manufacturing. An explainable machine learning method is used in this framework for modeling based on the frequency response data from the antenna sensor. In this approach, the explainable dimension reduction method can interpret the chosen components using projection matrix. The decision tree regressor exhibits proficiency in efficiently handling small datasets and retaining commendable explainability.

Experiments demonstrate that the S-parameter prediction generated by our method are more accurate and reliable. This method can be generalized to a new dataset.

Our work could provide a useful tool for antenna sensor modeling and signal processing fields during additive manufacturing.

Keywords: Additive manufacturing; Explainable AI; Machine Learning

#### I. Introduction

Machine learning (ML) holds significant potential to revolutionize the world of smart manufacturing. It can learn patterns within immense data reserves to perform intricate predictions on multiple flexible parameters [1]. Through the employment of ML, manufacturers can optimize complex processes, enhance product quality, minimize costs, predict malfunctions, and facilitate autonomous decision-making [2].

However, despite the prodigious capabilities of ML, full deployment in recommender systems, fault detection, quality control, predictive maintenance, etc., in the era of Industry 4.0 remains a significantly comprehensive and arduous goal [3] [4].

The intersection of ML and additive manufacturing (AM). also known as 3D printing, is a burgeoning field of research that promises to revolutionize the manufacturing industry. The application of ML techniques in additive manufacturing processes is increasingly becoming a focal point for researchers and industry professionals. This integration is pivotal in enhancing predictive modeling, real-time monitoring, and quality control within the AM processes [5]. Recent advancements in ML algorithms have shown significant potential in improving the precision, efficiency, and adaptability of additive manufacturing systems, particularly in complex tasks like antenna sensor modeling, as highlighted in the development of an explainable AI framework for antenna sensor modeling [6]. This framework not only ensures accurate predictions in the manufacturing process but also emphasizes the importance of interpretability in AI-driven decisions. The current research landscape is exploring these dual aspects - the enhancement of manufacturing capabilities through ML and the critical need for explainability in AI applications in AM.

However, as this technological convergence deepens, several critical issues have emerged, as documented in a growing body of literature. One of the primary challenges is the integration of ML algorithms with the complex and often unique processes inherent to AM, which requires not only sophisticated computational strategies but also a deep understanding of the physical principles of manufacturing [7]. Another significant issue is

National Science Foundation

data management and processing; the vast amounts of data generated during AM processes necessitate robust and efficient ML algorithms capable of real-time analysis and decision-making [8]. This is further complicated by the need for precision and reliability in AM, where even minor inaccuracies can lead to significant defects, particularly in critical applications like aerospace [9] and medical device manufacturing [10]. Additionally, there is the challenge of ensuring that the ML models used are interpretable and transparent, as the 'black box' nature of many ML algorithms can lead to trust and validation issues, especially in industries where certification and standard compliance are mandatory [11].

This paper seeks to delve into these emerging trends, examining how machine learning innovations are shaping the future of additive manufacturing, and addressing the challenges and opportunities that lie ahead. The contributions of our work are as follows.

- Development of a novel cylindrical resonator-based antenna sensor design specifically tailored for additive manufacturing applications.
- Proposition and implementation of an explainable AI method to visualize PCA dimension reduction, effectively elucidating component interactions in a low-dimensional space.
- Training of a decision tree regression model on a simulation dataset for the resonator antenna, achieving a substantial reduction in computation time and complexity compared to traditional simulation software.

The remainder of this paper is organized as follows: A literature review of related work is presented in Section II. We present the methodology in Section III. The evaluation is presented in Section IV. The conclusion and discussion are in Section V.

## II. RELATED WORK

Current efforts aim at increasing the explainability of machine learning methods used in additive manufacturing. Accordingly, current research addresses approaches to apply machine learning methods in resonator-based sensor modeling [add reference], and to find defects in additive manufacturing [11]. Since this research is utilized and closely related to our approach, we discuss these efforts in the following.

Resonator-based sensors used in additive manufacturing: The field of AM has seen a substantial integration of advanced sensor technologies, particularly resonator-based sensors, to enhance precision, monitoring, and quality control in manufacturing processes. A notable contribution in this area is by [12], who explored the use of microwave resonator sensors for real-time monitoring of 3D printing processes, highlighting their effectiveness in detecting material properties and structural anomalies. Building on this, the work of Peng, Xing, et al [13] demonstrated how resonator sensors could be adapted for temperature monitoring in AM, providing critical insights into thermal dynamics during printing. Furthermore, Fieber, Lukas, et al [14] delved into the application of acoustic resonator sensors in layer-wise monitoring, showcasing their

potential in detecting defects and layer thickness variations. These resonator-based approaches represent a significant shift towards more intelligent and adaptive AM processes.

Machine learning in resonator-based sensors: The incorporation of ML modeling with resonator-based sensors represents a burgeoning research area, especially in fields requiring precise measurement and monitoring. A notable study by Kazemi et al. [15] demonstrated the use of ML algorithms to model the frequency response of microwave resonators for material property detection, achieving high accuracy in identifying different materials based on their dielectric properties. Expanding this approach, Rooney [16] employed neural networks to interpret the data from acoustic resonator sensors, significantly improving the detection and classification of mechanical defects in manufacturing settings. Furthermore, the review [17] on current technology of microwave, fiber optical, and other resonator sensors using ML models showcased the ability to detect changes in environmental conditions, highlighting the potential for these sensors in monitoring applications.

Explainable Artificial Intelligence (xAI): The most current research are focusing on visual explanation for deep neural networks. Visual explanation methods such as Grad-CAM [18], NoiseCAM [19], and Local Interpretable Model-Agnostic Explanations (LIME) [20] provide visually understanding on the decision making of black-box models. Grad-CAM and NoiseCAM can generate a heatmap with different color in different area of the data. These colors can explain the contribution of colored area of the data to the model decision. Grad-CAM or NoiseCAM and other visual explanation methods enables the identification of regions that positively or negatively influence a particular prediction and quantifies the extent of their impact on the decision-making process [21].

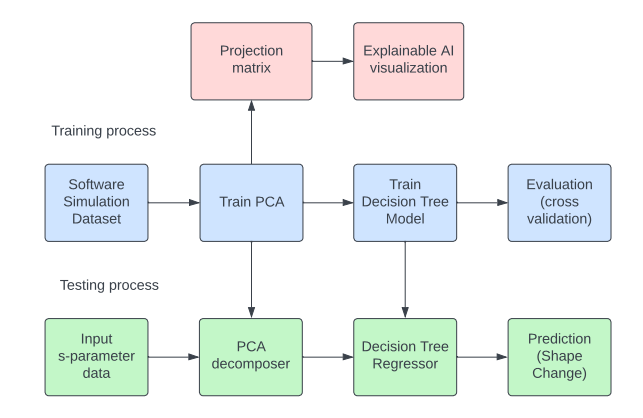


Figure 1. Embedded passive mmWave resonator antenna modeling analysis procedure

# III. METHODOLOGY

# A. Problem Definition

In order to correctly and efficiently use machine learning algorithm to model the signal response by embedded passive mmWave resonator sensor antenna for AM, it is crucial to understand several key components involved in this process.

These include the design and simulation of the antenna sensor, and the types of explainable AI algorithms best suited for this application. To achieve this, we provide a design of resonator antenna for in-plane embedding. Mean while, we utilize explainable AI techniques to analyze the dimension reduction and the regression prediction process of the trained model. Figure 1 provides a concise overview of our method for problem analysis.

# B. Antenna Design and Simulation

The Cylindrical Resonator utilizes a high permittivity material to attain resonance with high-quality factors at specified frequencies. To achieve this, a resonator was constructed using ceramic-loaded polyvinylidene fluoride (PVDF) with a permittivity of Er=10. This PVDF cylinder was encased within a metallic jacket to confine the resonance within the cylinder and minimize energy loss rates [22]. Essentially, this structure operates as a circular cavity resonator, where the PVDF material serves as the dielectric filling the cavity. The dimensions of the cylinder can be estimated using the formula:

$$a = \frac{c}{2\pi f_r \sqrt{E_r}} \sqrt{p_{mn\_first\_order}^2 + (\frac{\pi}{L_{by\_a}})^2}$$
 (1)

where  $p_{mn} = 3.832$ ;  $L_{by\_a} = 2$ .

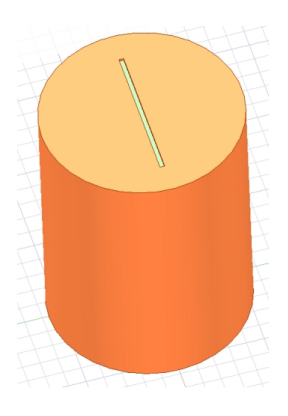


Figure 2. Cylindrical Resonator Slot Antenna Sensor

The slot antenna is etched onto the flat surface of the Cylindrical Resonator, specifically on the metallic layer without affecting the dielectric. This slot antenna was tailored for operation at 30GHz and finely tuned to align with the resonance of the PVDF cylinder. Base on [23], the dimensions of the slot antenna were determined as follows

$$\frac{L}{\lambda_0} = \frac{L_0}{\sqrt{\frac{\epsilon_r + 1}{2}}} \tag{2}$$

where  $L_0$  is the length for  $\epsilon_r = 1$ .

Fig 2 is the 3D model of the cylindrical resonator slot antenna sensor.

The simulation of the Cylindrical Resonator Slot Antenna Sensor took place in Ansys HFSS to collect data for machine learning. A frequency domain analysis was conducted using a Radiation boundary setup and a Wideband horn antenna as the probing antenna. The details of the simulation setup are illustrated in Fig 3.

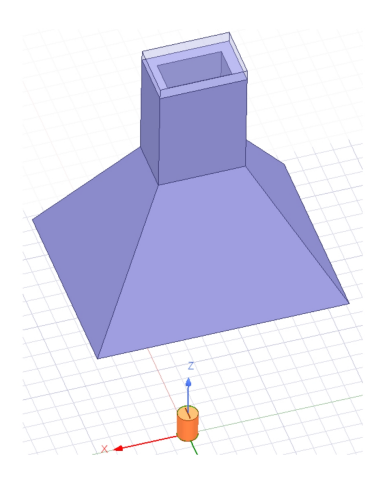


Figure 3. Simulation Setup in Ansys HFSS

## C. Explainalbe PCA Dimension Reduction

Principal component analysis (PCA) [24] are widely applied on variance domain. The dimension reduction ability of PCA has been proofed and used across years [25]. We use PCA to reduce the dimension of each sample from the dataset we collected by simulation on sector III-B.

To reduce the dimension of the data, PCA finds low dimensional approximations by projecting the data onto subspace. The principal subspace in dimention k is compute as

$$s_k = \operatorname{argmin} E(\min ||\hat{X} - y||^2)$$
 (3)

where  $\mu = E(X)$  and  $\hat{X} = X - \mu$ . It has the covariance matrix Cov(X) compute as

$$Cov(X) = E((X - \mu)(X - \mu)^T)$$
(4)

Then we can obtain the eigenvalue  $\lambda_1, \lambda_2, ..., \lambda_d$  and the eigenvector  $[e_1, e_2, ..., e_d]$  of the covariance matrix Cov(X).

The dimension reduced version of X is

$$T_k(X) = \mu + \sum_{i=1}^{k} \beta e \tag{5}$$

where  $\beta = \langle X - \mu, e \rangle$ , e is eigenvectors of the covariance matrix, and  $\sum^k \beta e$  is the projection matrix of X onto  $s_k$ . When we choose first m principal components, the percentage of variance can be calculate as

$$Var = \frac{\sum^{m} \lambda}{\sum^{d} \lambda} \tag{6}$$

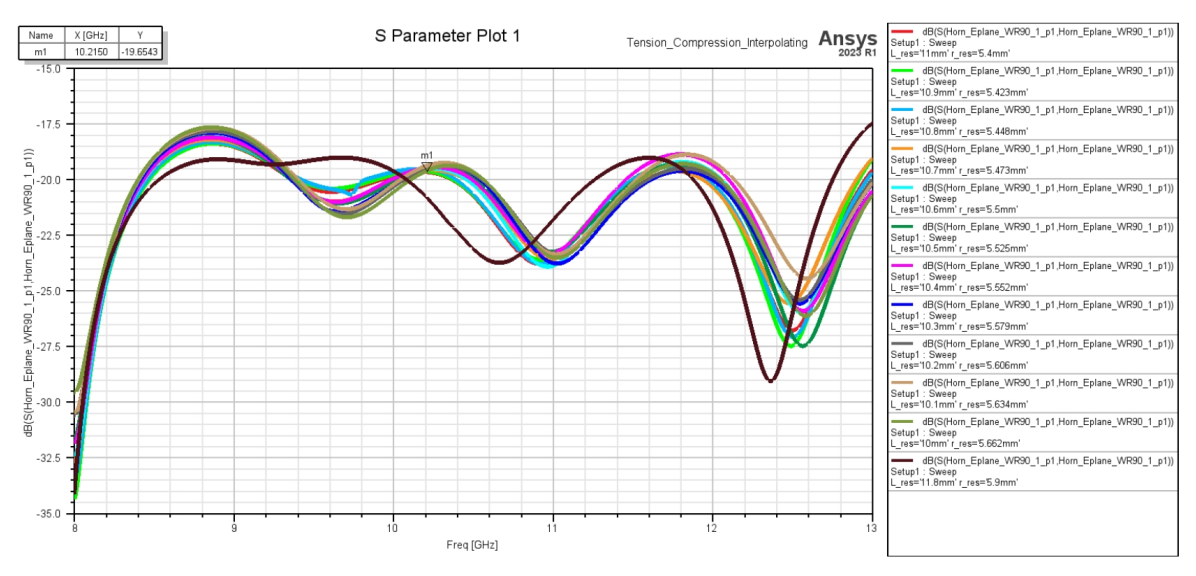


Figure 4. S11 - Tension Compression

To explain the behavior of the PCA method on dimension reduction and the meaning and representation of the chosen first m principal components, we obtain the projection matrix  $\sum^k \beta e$  from the matrix transforming, and visualize it in a RGB image. The evaluation and visualization are shown on IV-B.

# D. Decision Tree Regression Modeling

The paper employs the Classification And Regression Tree (CART) algorithm [26], a versatile decision tree method proficient in both classification and regression tasks within machine learning. CART serves as a predictive model elucidating the prediction of the target variable's value through the training dataset. It operates as a decision tree, where each branch denotes a predictor variable and each node provides a prediction for the final target variable. In this study, a regression trees algorithm based on CART is utilized to predict the continuous variables linked to the change in the cylindrical antenna.

CART algorithm uses Gini Impurity to split the dataset into a decision tree. It does that by searching for the best homogeneity for the sub nodes, with the help of the Gini index criterion. The Gini Impurity can compute as follow

$$Gini(P) = 1 - \sum_{i=1}^{n} (p_i)^2$$
 (7)

where  $P = (p_1, ..., p_i)$  is the probability of an object going to a particular node. Base on the formula of information gain, we calculate the IG in our model as follow

$$GiniGain_{Y}(X_{i}, D) = GiniBeforeSplit - GiniAfterSplit$$

$$= Gini(P_{y}(D)) - \sum_{j=1}^{m} \frac{|\sigma_{X_{i}=v_{j}}(D)|}{|D|} Gini(P_{Y}(\sigma_{X_{i}=v_{j}}(D)))$$
(8)

where D donate as the dataset, and  $\sigma_{X_i=\nu_j}(D)$  is the subset after splitting.

### IV. EVALUATION

This section presents the simulation results of our cylindrical resonator-based antenna sensor design. Further more, it examines the regression model trained by collected dataset from simulation of our cylindrical resonator-based antenna sensor. The goal is to generate a fit regression model for this antenna sensor. Moreover, we provide a visual explanation on dimension reduction and decision making process.

# A. Dataset from Simulation

We use Ansys to simulate our resonator-base antenna design. Figure 5 illustrates significant E-field concentrations on the cylinder's surface at the slot, indicating a coupling between the resonator and the slot antenna. As depicted in Figure 6, the horn antenna detects a reflection from the resonator slot antenna, and the corresponding S11 parameter differs when the resonator is present compared to its absence. The sensor's embedding within a structure leads to changes in its dimensions in response to the structure's deformation, owing to the sensor material's elasticity. This deformation effect is quantifiable by comparing the sensor's reflected parameters in its deformed state to the baseline case, allowing the determination of the structure's strain. Figure 4 displays the horn antenna's reflections for varying sensor dimensions that represent different tension-compression scenarios. Each scenario yields a distinct S11 value, which can be analyzed by a computer algorithm to deduce the corresponding dimensions and, consequently, the stress-strain values.

## B. Explaination on PCA method

Using the methods in Section IV-B, we found that the dimension of our collected dataset can be reduced from 501 to 3. The cumulative explained variance reach 95.20%. We also obtained the projection matrix  $\sum^{k} \beta e$  to explain the component after dimension reduction.

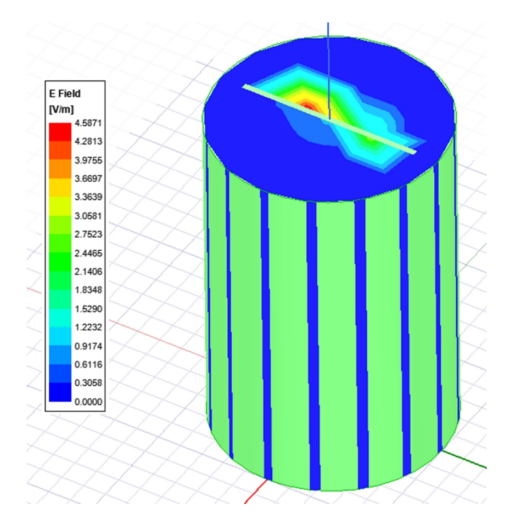


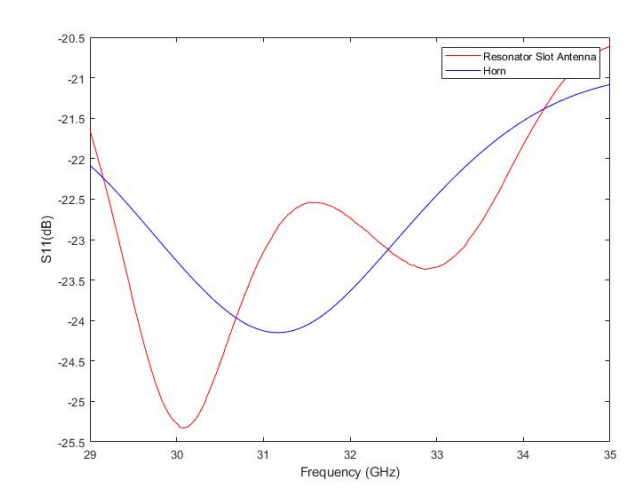
Figure 5. Resonator E-Field

Table I. PCA Overview

Number of Com-	Explained Variance	Cumulative		
ponents				
1	0.783899	0.783899		
2	0.122060	0.905960		
3	0.046120	0.952079		
Mean Explained Variance: 0.317				

According to Table I, the first component can explain 78.38% of the variance of the dataset, the second and third components explain 16.82% variance. Although the second and third components only explain a small amount of variance, it is important that they act as a support component to fully explain the whole dataset. Based on this observation, we consider that the first component will dominant the decision making of the model on the dataset after dimension reduction. This conjecture will be proofed by our experiment result on Section IV-C.

The projection matrix  $\sum^{k} \beta e$  is a 3 rows by 501 columns



**Figure 6.** This figure need to re-generate, make lines bold and clear, text font larger, legend clear. S11 - Horn Reflection Parameter

matrix. This matrix reflects the projection space of the PCA transform, and it can be visualized to explain the focus frequency bandwidth of each component, as shown in Figures 7. The red line is 0 weight, the peak area on each component indicates the focus frequency bandwidth in PCA transforming. However, we do notice some unfocused bandwidths, which indicates that those frequency bandwidths are unnecessary to distinguish the variance on the dataset. For example, the 8.5 Ghz to 10.6 Ghz and 11.2 Ghz to 12.4 Ghz in the second component projection vector, those bandwidth will be assigned 0 weight in PCA dimension reduction.

## C. Performance of Decision Tree Regression Modeling

In our study, a decision tree regression model was trained using a dataset subjected to PCA for dimensionality reduction. The model's performance was assessed through K-fold cross-validation, specifically employing 10 folds, as indicated in Table II. This approach yielded an average root mean squared error of 0.055 for the model.

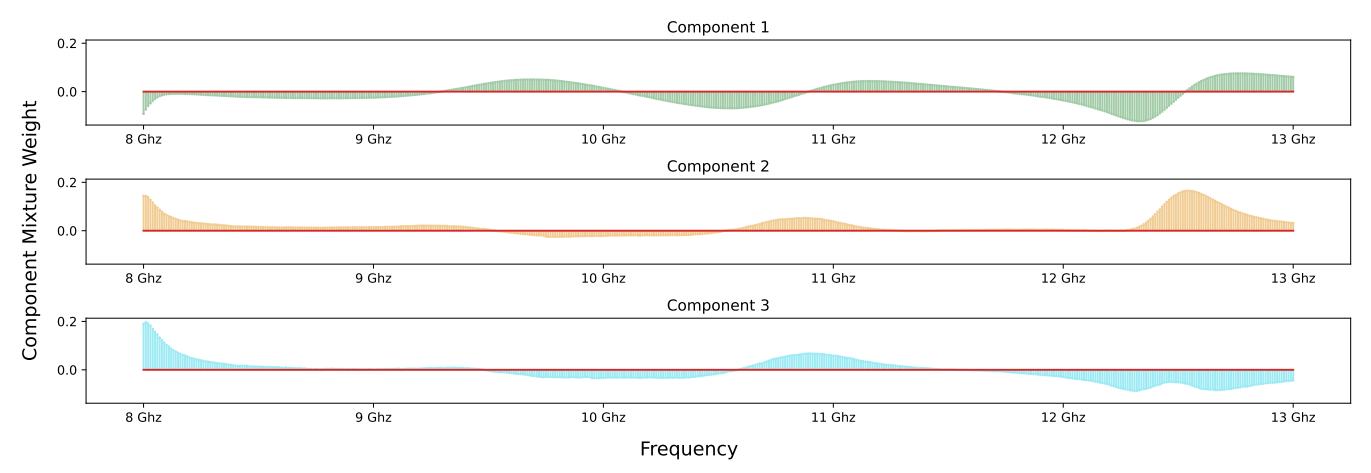


**Figure 7.** Explainable Visualization of Projection Matrix  $\sum^{k} \beta e^{-\beta t}$ 

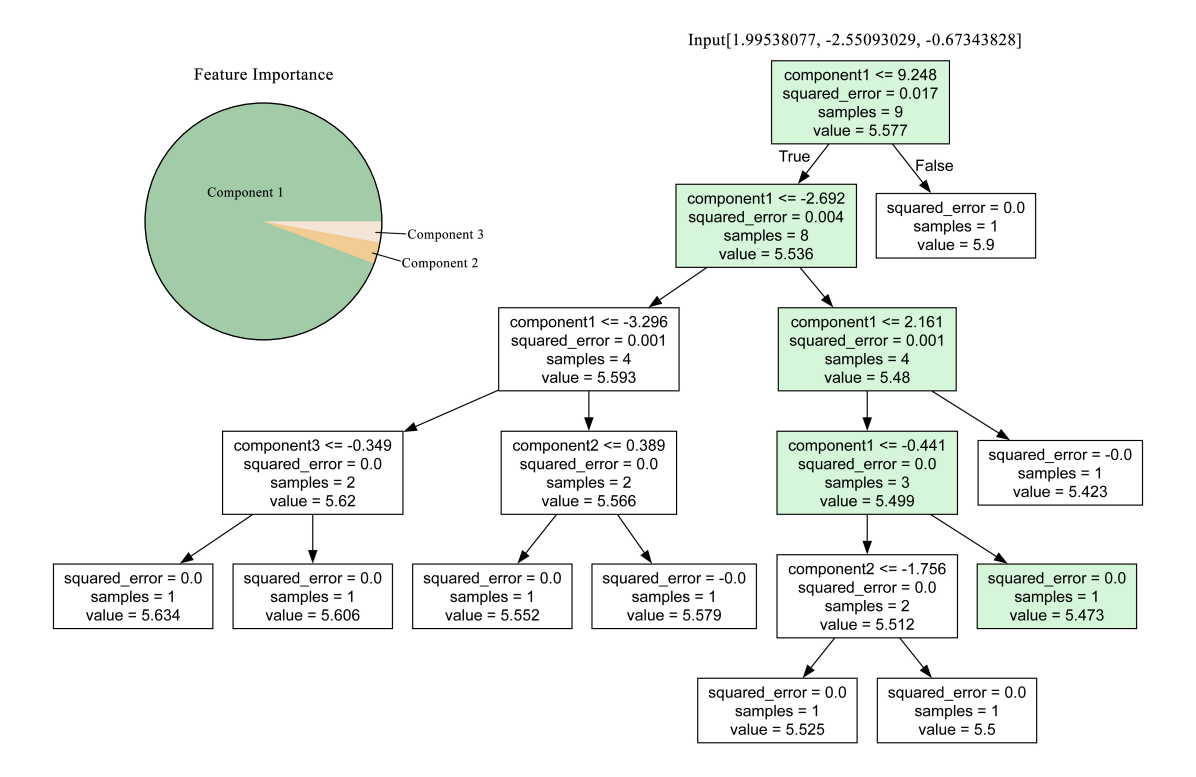


Figure 8. Decision Tree and Feature Importance Visualization

We have shown the quantitative comparison on different methods in Table III. The RMSE result demonstrate that the s-parameter generated by our method are more accurate. With the explainable method, the result by our method are more reliable.

Table II. Cross Validation Score

RMSE of $ S_{11}  $					
Fold 1	Fold 2	Fold 3	Fold 4	Fold 5	
0.0365	0.0635	0.052	0.027	0.052	
Fold 6	Fold 7	Fold 8	Fold 9	Fold 10	
0.083	0.027	0.028	0.137	0.0477	
Average RMSE: 0.05537					

Table III. Performance Comparison

RMSE of $ S_{11}  $					
Method	MS-CoML [27](Best)	MS-CoML(Avg.)			
RMSE	0.0597	0.1019			
Method	GP Model [28]	ANN (40 nodes) [28]			
RMSE	0.19	0.18			
Method	Ours				
RMSE	0.05537				

A detailed visualization of the trained decision tree model is presented in Figure 8, demonstrating the model's decision-making process with reduced dimensionality to three principal components. This visualization not only simplifies the understanding of the model's functioning but also highlights the significance of the components, with Component 1 emerging

as the most influential in decision-making. Components 2 and 3 play a supportive role in the model's decisions. These findings corroborate the earlier hypothesis discussed in Section IV-B, where Component 1 was identified as having the highest explained variance, thus playing a dominant role in the model's decision-making process.

## V. CONCLUSION AND FUTURE WORK

In this work, we provide a new design of cylindrical resonator-base antenna sensor for additive manufacturing. The functions of our antenna design have been proof by simulation on Ansys. We proposed an explainable AI method on visualizing the PCA dimension reduction, and this method successfully explains the components in low dimension space. We train a decision tree regression model on the simulation dataset of the resonator antenna, which significantly reduces the computation time and complex comparing to the simulation software. Going forward, we aim to extend our antenna design and machine learning model as an efficient tool for additive manufacturing with more types of physical sensing parameter.

#### ACKNOWLEDGMENT

This material is based upon work supported by the National Science Foundation under Grant No. 2229155. The opinions, findings, and conclusions, or recommendations expressed are those of the author(s) and do not necessarily reflect the views of the National Science Foundation.

#### REFERENCES

- Y. LeCun, Y. Bengio, and G. Hinton, "Deep learning," *nature*, vol. 521, no. 7553, pp. 436–444, 2015.
- [2] G. Fortino, C. Savaglio, G. Spezzano, and M. Zhou, "Internet of things as system of systems: A review of methodologies, frameworks, platforms, and tools," *IEEE Transactions on Systems, Man, and Cybernetics:* Systems, vol. 51, no. 1, pp. 223–236, 2020.
- [3] O. Z. Maimon and L. Rokach, Data mining with decision trees: theory and applications. World scientific, 2014, vol. 81.
- [4] J. Lee, B. Bagheri, and H.-A. Kao, "A cyber-physical systems architecture for industry 4.0-based manufacturing systems," *Manufacturing letters*, vol. 3, pp. 18–23, 2015.
- [5] M. Vaezi, H. Seitz, and S. Yang, "A review on 3d micro-additive manufacturing technologies," *The International Journal of Advanced Manufacturing Technology*, vol. 67, pp. 1721–1754, 2013.
- [6] S. K. Jagatheesaperumal, Q.-V. Pham, R. Ruby, Z. Yang, C. Xu, and Z. Zhang, "Explainable ai over the internet of things (iot): Overview, state-of-the-art and future directions," *IEEE Open Journal of the Com*munications Society, 2022.
- [7] J. Qin, F. Hu, Y. Liu, P. Witherell, C. C. Wang, D. W. Rosen, T. W. Simpson, Y. Lu, and Q. Tang, "Research and application of machine learning for additive manufacturing," *Additive Manufacturing*, vol. 52, p. 102691, 2022.
- [8] Y. Zhang, M. Safdar, J. Xie, J. Li, M. Sage, and Y. F. Zhao, "A systematic review on data of additive manufacturing for machine learning applications: the data quality, type, preprocessing, and management," *Journal of Intelligent Manufacturing*, vol. 34, no. 8, pp. 3305–3340, 2023.
- [9] M. Khorasani, A. Ghasemi, B. Rolfe, and I. Gibson, "Additive manufacturing a powerful tool for the aerospace industry," *Rapid prototyping journal*, vol. 28, no. 1, pp. 87–100, 2022.
- [10] M. P. Francis, N. Kemper, Y. Maghdouri-White, and N. Thayer, "Additive manufacturing for biofabricated medical device applications," in *Additive manufacturing*. Elsevier, 2018, pp. 311–344.
- [11] D. Kumar, Y. Liu, H. Song, and S. Namilae, "Explainable deep neural network for in-plain defect detection during additive manufacturing," *Rapid Prototyping Journal*, 2023.
- [12] S. Mohammadi, A. V. Nadaraja, D. J. Roberts, and M. H. Zarifi, "Real-time and hazard-free water quality monitoring based on microwave planar resonator sensor," *Sensors and Actuators A: Physical*, vol. 303, p. 111663, 2020.
- [13] X. Peng, L. Kong, Y. Chen, Z. Shan, and L. Qi, "Design of a multi-sensor monitoring system for additive manufacturing process," *Nanomanufacturing and Metrology*, vol. 3, pp. 142–150, 2020.
- [14] L. Fieber, S. S. Bukhari, Y. Wu, and P. S. Grant, "In-line measurement of the dielectric permittivity of materials during additive manufacturing and 3d data reconstruction," *Additive Manufacturing*, vol. 32, p. 101010, 2020
- [15] N. Kazemi, N. Gholizadeh, and P. Musilek, "Selective microwave zerothorder resonator sensor aided by machine learning," *Sensors*, vol. 22, no. 14, p. 5362, 2022.
- [16] S. Rooney, "Ai for state estimation and diagnostics of additive manufacturing machinery," Ph.D. dissertation, Stevens Institute of Technology, 2023
- [17] Z. Fan, R. X. Gao, Q. He, Y. Huang, T. Jiang, Z. Peng, L. Thévenaz, Y. Xiong, S. Zhong et al., "New sensing technologies for monitoring machinery, structures, and manufacturing processes," *Journal of Dynamics*, Monitoring and Diagnostics, 2023.
- [18] R. R. Selvaraju, M. Cogswell, A. Das, R. Vedantam, D. Parikh, and D. Batra, "Grad-cam: Visual explanations from deep networks via gradient-based localization," in *Proceedings of the IEEE International* Conference on Computer Vision (ICCV), Oct 2017.
- [19] W. Tan, J. Renkhoff, A. Velasquez, Z. Wang, L. Li, J. Wang, S. Niu, F. Yang, Y. Liu, and H. Song, "Noisecam: Explainable ai for the boundary between noise and adversarial attacks," arXiv preprint arXiv:2303.06151, 2023.
- [20] M. T. Ribeiro, S. Singh, and C. Guestrin, "" why should i trust you?" explaining the predictions of any classifier," in *Proceedings of the 22nd ACM SIGKDD international conference on knowledge discovery and data mining*, 2016, pp. 1135–1144.
- [21] D. Cian, J. van Gemert, and A. Lengyel, "Evaluating the performance of the lime and grad-cam explanation methods on a lego multi-label image classification task," arXiv preprint arXiv:2008.01584, 2020.

- [22] B. C. A., "Advanced engineering electromagnetics," pp. 352-548, 2012.
- [23] T. Weller, L. Katehi, and G. Rebeiz, "Single and double folded-slot antennas on semi-infinite substrates," *Antennas and Propagation, IEEE Transactions on*, vol. 43, pp. 1423 – 1428, 01 1996.
- [24] A. Maćkiewicz and W. Ratajczak, "Principal components analysis (pca)," Computers Geosciences, vol. 19, no. 3, pp. 303–342, 1993.
- [25] N. Salem and S. Hussein, "Data dimensional reduction and principal components analysis," *Procedia Computer Science*, vol. 163, pp. 292– 299, 2019, 16th Learning and Technology Conference 2019Artificial Intelligence and Machine Learning: Embedding the Intelligence.
- [26] C. J. S. R. O. Leo Breiman, Jerome Friedman, Classification and Regression Trees. Chapman and Hall/CRC, 1984.
- [27] Q. Wu, H. Wang, and W. Hong, "Multistage collaborative machine learning and its application to antenna modeling and optimization," *IEEE Transactions on Antennas and Propagation*, vol. 68, no. 5, pp. 3397–3409, 2020.
- [28] Y. Sharma, X. Chen, J. Wu, Q. Zhou, H. H. Zhang, and H. Xin, "Machine learning methods-based modeling and optimization of 3-dprinted dielectrics around monopole antenna," *IEEE Transactions on Antennas and Propagation*, vol. 70, no. 7, pp. 4997–5006, 2022.